united nations
educational, scientific
and cultural
organization

international atomic
energy agency

the
abdus salam
international centre for theoretical physics

SMR/1270-12

SCHOOL ON SYNCHROTRON RADIATION

6 November - 8 December 2000

Miramare - Trieste, Italy

Supported in part by the Italian Ministry of Foreign Affairs in connection with the SESEME project

Co-sponsors: Sincrotrone Trieste, Società Italiana di Luce di Sincrotrone (SILS) and the Arab Fund for Economic and Social Development

Gratings and Mirrors

D. Cocco
Sincrotrone Trieste
Italy

Gratings and Mirrors

Daniele Cocco

Sincrotrone Trieste

School on Synchrotron Radiation

6 Novembre – 8 December 2000

Miramare – Trieste ITALY

Materials and manufacture

One of the major advantages of Synchrotron Radiation (SR) sources, is their ability to provide high brilliance photons in the soft x-ray region. This part of the electromagnetic spectrum is of great interest, because many materials have strong absorption edges at these energies. If one is able to monochromate these photons, the chemical state of atoms and molecules can be studied in depth, and consequently their interaction behaviour understood.
Unfortunately, from the point of view of the optics, this strong absorption is a disadvantage. As a matter of fact, the absorption properties of the materials make impossible the use of ordinary normal incidence optics schemes. Therefore one is forced to work in grazing incidence configurations. Mirror reflectivity decreases dramatically with increasing photons energy and incidence angle. For this reason, grazing incidence angles of 2 degrees or lower, are usually adopted by the SR beamline designers.
The typical shapes for synchrotron mirrors and gratings vary from plane to the more exotic aspherical forms (e.g. paraboloid, ellipsoid, toroids, and so on). Moreover, the parameters of these mirrors are rather variable. Ellipsoidal and toroidal optical surfaces, with radius (or equivalent radius) of curvature from 10 or 20 metres, up to some kilometres in the tangential direction, and close to a few centimetre in the sagittal one, are typically specified.
On the other hand, for such small incidence angles, every imperfection on mirrors and gratings optical surfaces, will result in drastically reduced overall performance of a multi-component beamline, designed to monochromate and focus synchrotron light.
Deviations from the ideal slope of a few μRad RMS, and surface roughness exceeding few Å RMS, might be sufficient to reduce substantially both, the energy resolution and the photon density required for the experiments. The boundary between roughness (i.e. microscopic deviation from the ideal optical surface) and slope errors (deviations with period of the order of the mm of larger) is quite ambiguous. Typically one can say that every error on the shape that could be described with a polynomial series with periods below half a millimetre is roughness and above a couple of mm is slope error. Nevertheless, the zone between 0.5 and 2 mm is important too for the performance of the optics and therefore, the manufactures try to enlarge the gap and the customers to reduce it.
Both the gratings and the mirrors could be made, in principle, by the same materials. The main problem is to found a material which could be polished and treated opportunely to produce the required shape with the required precision and in the mean time, this material have to satisfy some requirements. First of all, the materials have to be UHV compatible, have to have a limited thermal expansion (to avoid deformation under the synchrotron radiation beam) have to be rigid enough to do not be deformed by the clamping system and, in many cases, it must be cooled.
Depending on the material chosen, the roughness and the slope errors could be reduced to acceptable values.
Some widely used materials are summarised in the following table:

Material	Density	Young's modulus	Thermal expansion	Thermal conductivity	Figure of merit
	Gm/cc	GPa	(α) ppm/°C	(k) W/m/°C	k/α
Silicon	2.33	131	2.6	156	60
Silicon Carbide	3.21	461	2.4	198	82.5
Glidcop	8.84	130	16.6	365	22
Molybdenum	10.21	324	4.8	142	29.6
Fused silica	2.17	73	0.5	1.4	2.8
Zerodur	2.53	92	0.05	1.6	32

From this table, it is evident that Silicon Carbide (SiC) is a good material when one need to cool the mirror/grating. It is in fact rigid enough to do not be deformed by the clamping and has a high figure of merit, i.e. a limited thermal expansion together with a good thermal conductivity. It means that with a cooling system made by a cool object put in tight contact with the edge of the optics, it's possible to dissipate the heat induced by the synchrotron radiation light.
Another advantage of its stiffness is the fact that is possible to polish it with a very good surface finishing. It means that the final roughness could be of the order of 0.1nm rms. The same statement is valid for Silicon and glass material in general, while for metal this is not true. As a matter of fact, the metals are typically malleable, and therefore, the friction with the polishing tools produce always some particles of materials, which damage the surface.
If one need to cool the optics, another possible solution is the use of Glidcop, Copper or Molybdenum, but with the option of the internal cooling.
Since we are dealing with metals we are able to weld its. In reality the procedure of welding is a little bit complicated and must be vacuum compatible and is called "braze".
Nevertheless, it is possible to create some channel close to the optical surface inside the blank and let the water circulate inside it. Therefore, even if the thermal conductivity of the material is poorer respect silicon or SiC, the cooling channel are very close to the optical surface and the cooling procedure is efficient too.

To increase the reflectivity of the mirrors or the efficiency of the gratings, a coating is used. It consist in the deposition (made in different ways) of a particular material above the polished optical surface. In this way the radiation (that never penetrates a material for a depth larger than some nm) meet only the coating and the reflectivity is due only to the coating characteristics.
The choice of the coating depends on the energy of the photons one wish to use. In normal incidence mode, in the UV range, a typical coating is Aluminium with a MgF_2 over-coating to protect the aluminium from the oxidation. In the lower part of the Soft X-ray radiation, good choice is Carbon, Gold, Nickel, Platinum and some other metallic layers. Nevertheless, when the higher energy are necessary, only gold and platinum become good choice, due to the absence of absorption edges in the soft x-ray range.
In the following the reflectivity of some typically used material is reported. The reflectivity is calculated at 2° of grazing incidence angle.

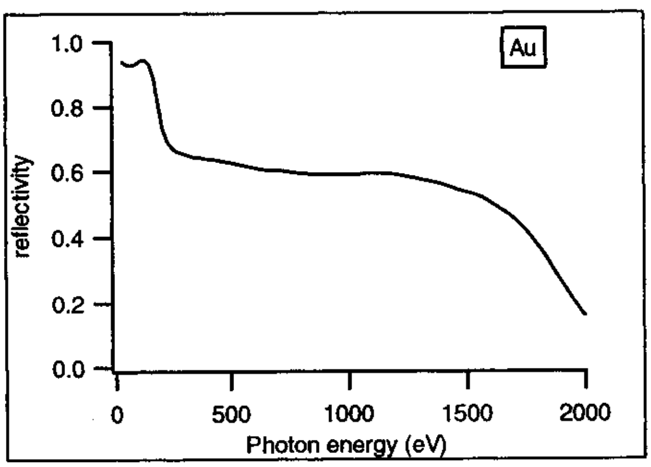

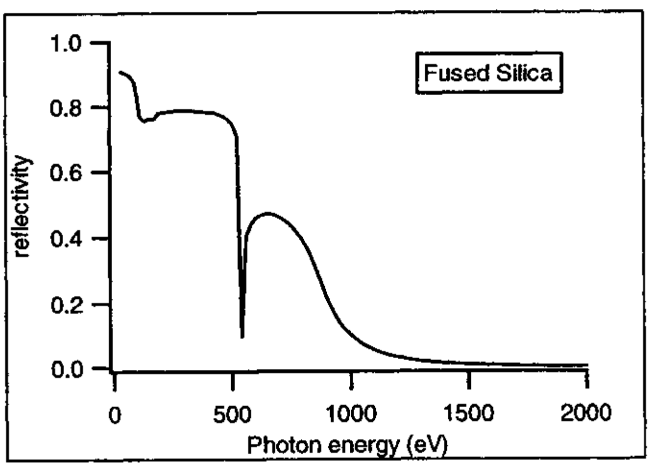

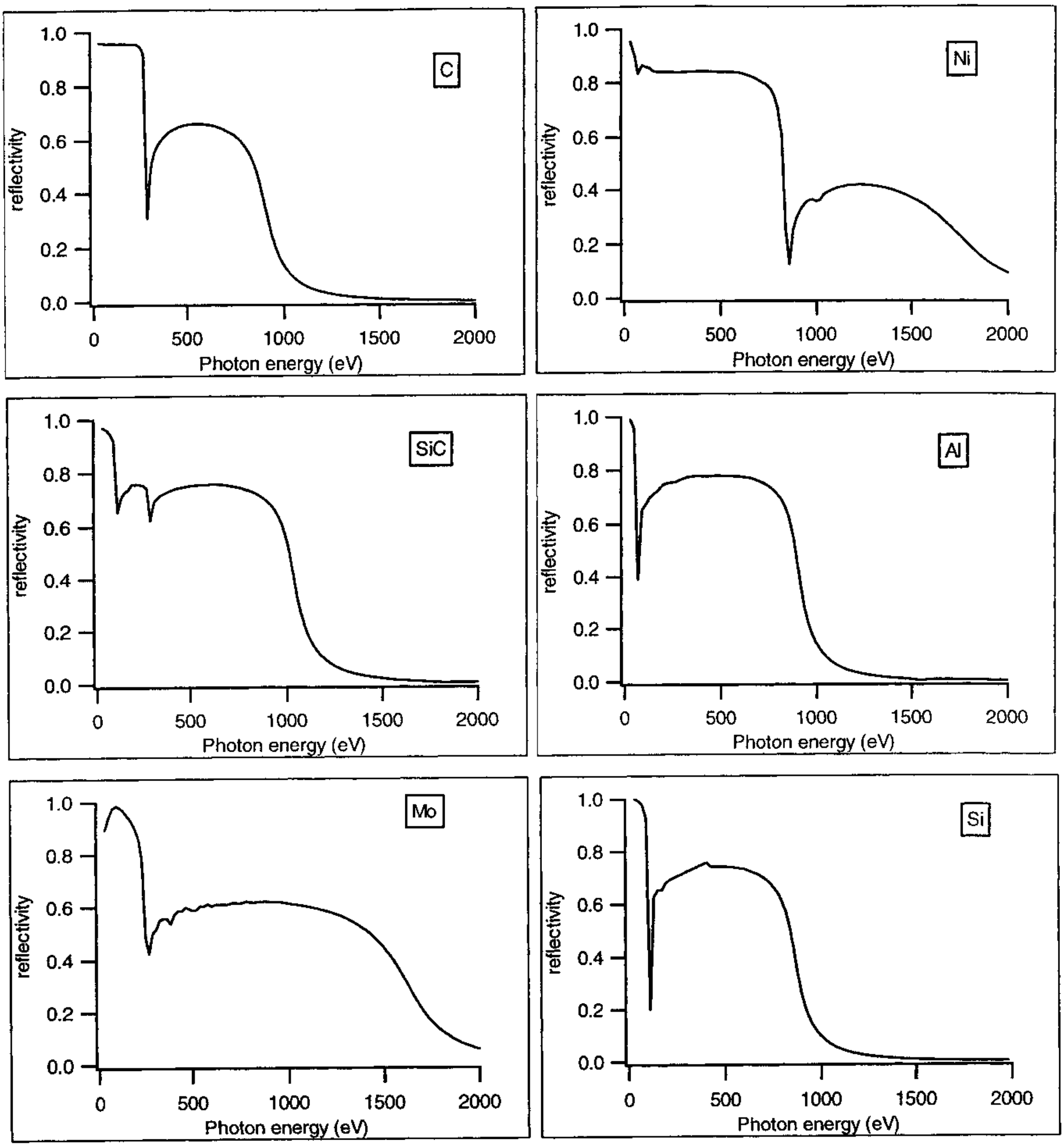
C
reflectivity
Photon energy (eV)
Ni
reflectivity
Photon energy (eV)
SiC
reflectivity
Photon energy (eV)
Al
reflectivity
Photon energy (eV)
Mo
reflectivity
Photon energy (eV)
Si
reflectivity
Photon energy (eV)
0.0 0.2 0.4 0.6 0.8 1.0
0 500 1000 1500 2000

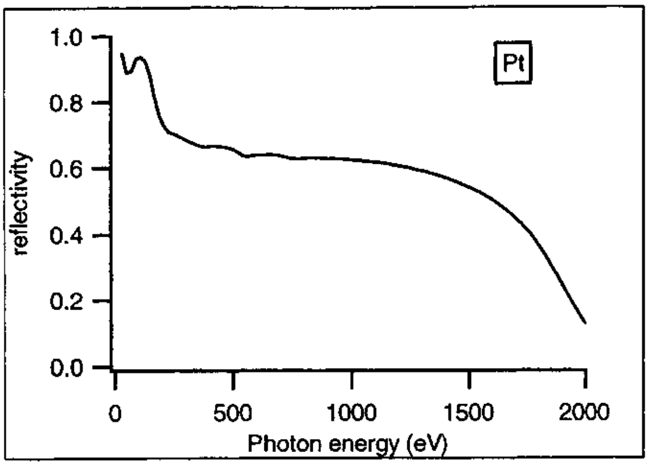

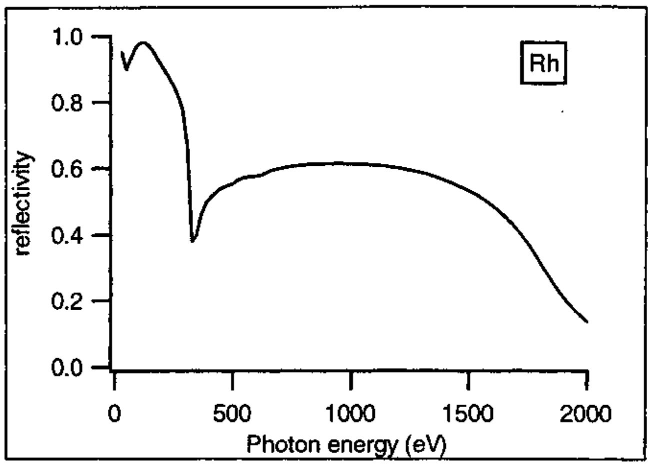

From these graphics, is evident that Au e Pt are quite good in the whole range while, for instance, Nickel is good up to 700 eV and at lower energy the choice is rather big.

The behaviour of the reflectivity with the angle of incidence is quite obvious. Since the penetration depth of the photons into the matter increase, the absorption increases too. For this reason higher is the angel of incidence lower is the reflectivity.
In the following graph the reflectivity of gold as a function of the photon energy is reported for different angle of incidence.

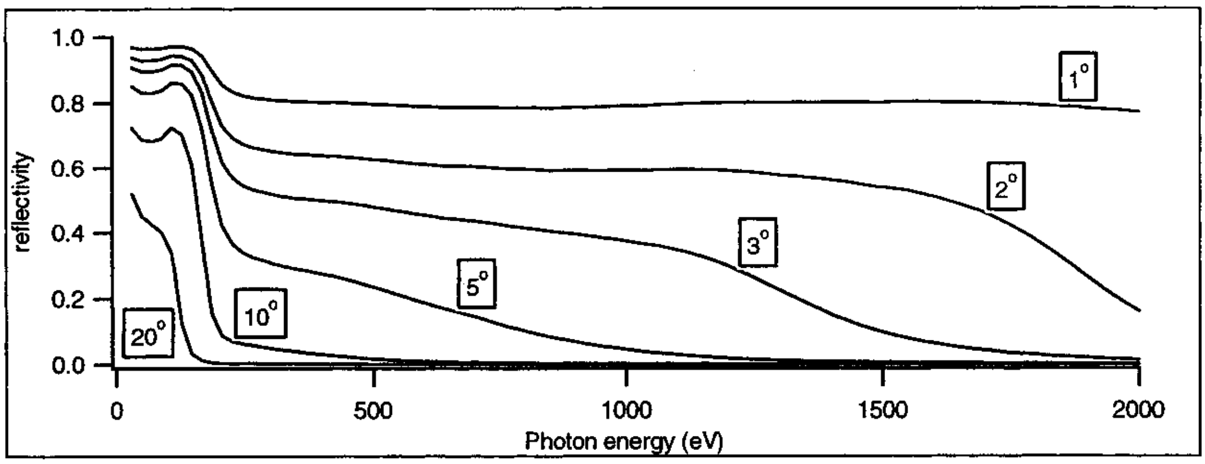

Figure errors

As previously mentioned, the error on the optics surface could be divided into two groups. The errors with period of the order of the millimetre (slope errors) and that ones with very small period (roughness)
The slope errors could be thought as imperfections that locally change the direction of the normal to the optical surface and therefore change the direction of the reflected radiation. In the following drawn $\delta\theta$ is the change in the normal direction and $2\delta\theta$ (since the angle is doubled by the reflection) is the change in the reflected beam.

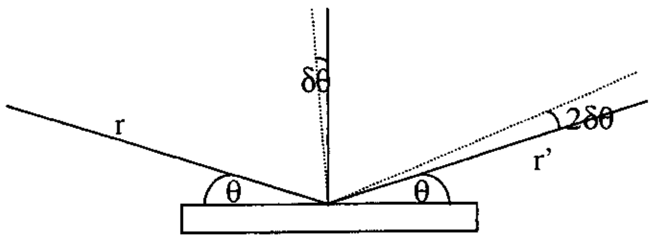

The plane drawn here is the so-called tangential plane. This is the plane designed by the normal to the optical surface and the incoming radiation. In this plane, the effect of the enlargement of the spot (s) at a distance r' from the mirror is easily estimated by:

$\Delta s = 2r'\delta\theta$ tangential

In the plane perpendicular to the tangential, the so-called sagittal plane, the effect of the enlargement is reduced. As a matter of fact, an error in the direction perpendicular to the incoming rays, only introduce a deviation for the vectorial component perpendicular to the surface. Therefore the enlargement of the spot in the sagittal direction could be estimated by:

$\Delta s = 2r'\delta\theta \sin(\theta)$ sagittal

The following two graphs show the enlargement of the spot due to the slope errors in both, the tangential and sagittal plane. In the first one r' is constant (1m) and the enlargement is plotted as a function of the slope error, in the second the slope error is fixed and the enlargement is plotted as a function of the distance from the mirror.

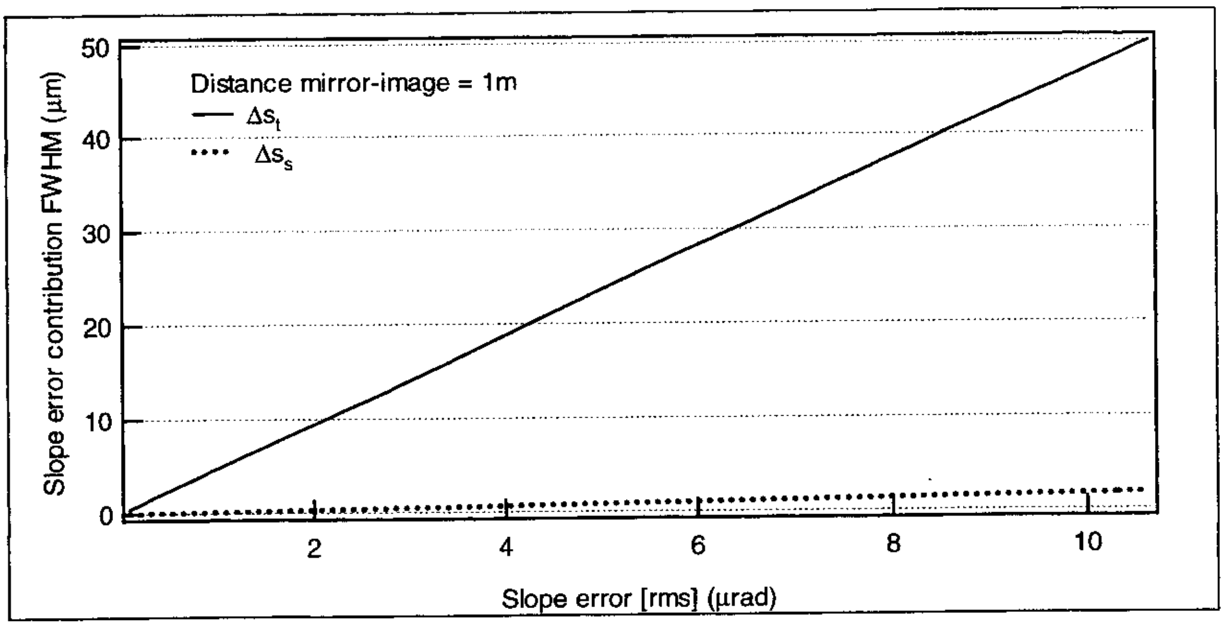

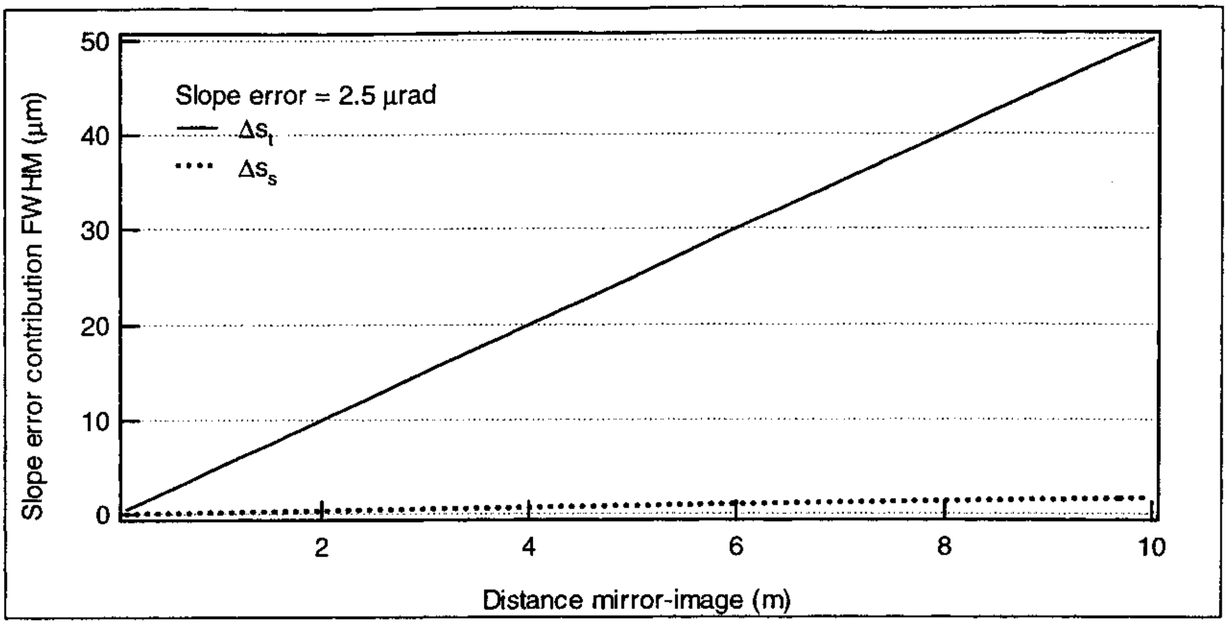

The second kind of error, the roughness, could be thought as a random distribution of small imperfection. In this way the final effect is a reduction of the intensity in the reflected peaks because the rays are dispersed all around the reflected beam direction and the dispersion profile follow a Gaussian distribution. The parameter of this gaussian profile depend from the ratio σ/λ where σ is the amplitude of the roughness and λ is the wavelength of the incoming radiation. Smaller is the wavelength higher is the effect of the roughness.

The intensity of the reflected radiation I is reduced with respect to the ideal reflected radiation intensity (I_0) by a factor proportional to the above mentioned ratio and precisely:

$$I = I_o e^{-\left(\frac{4\pi\sigma sin\vartheta}{\lambda}\right)^2}$$

Gratings

A diffraction grating, the heart of a Soft X-ray beamline, is an artificial periodic structure with a well defined period *d*. The incoming and outgoing radiation directions are related by a simple formula:

$$\frac{n\lambda}{d} = sin(\alpha) - sin(\beta) \tag{1}$$

where α is the angle of incidence and β is the angle of diffraction, both with respect to the normal (see next figure), n the diffraction order and λ the wavelength of the selected radiation.

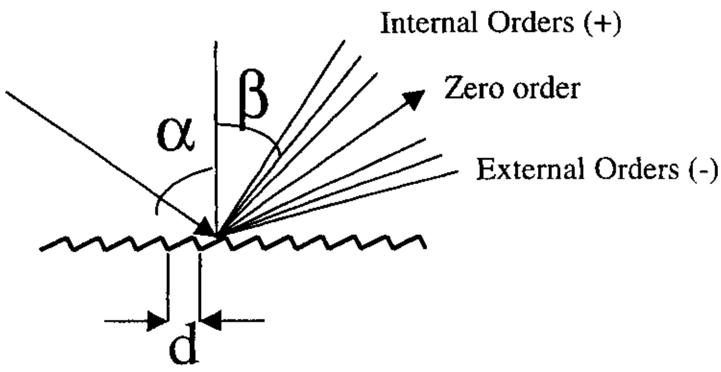

An alternative description of the same law is the following:

$$nK\lambda = sin(\alpha) - sin(\beta) \qquad (2)$$

where K=1/d is the groove density.
The profile of the grooves of the gratings could be sinusoidal (not often used), laminar or blaze.

Blaze

Laminar

The diffraction gratings can be produced by several ways. They can be mechanically ruled by means of a diamond tool that drills the substrate, holographically recorded and also replicated from a master. In all these cases some errors occur during the manufacturing process. These defects can be periodic (or quasi-periodic) or completely random. In any case, the final effect of these defects is a reduction of the ability of the grating to select the proper photon energy, the reduction of the photon flux (due, for instance, to the stray light) or the presence of unwanted diffracted energy together with the selected one (ghosts). In the next picture, below the rough presentation of the possible imperfections, a formula to estimate the intensity reduction due to the imperfections is reported.

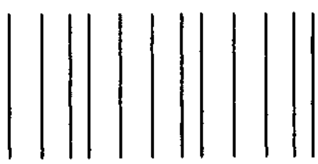

Periodic imperfections

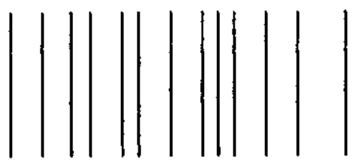

Random imperfections

$$I_g = I_0 \left(\frac{n\pi \ \delta d}{d} \right)^2$$

$$I = I_0 \exp - \left(\frac{2\pi \ sin\beta \ \delta d}{\lambda} \right)$$

δd is, in the periodic imperfection case, the maximum deviation from the ideal d-spacing, while in the random distributed case is the rms deviation from the ideal d-spacing.
The knowledge of these defects is as important as the knowledge of the slope errors of the substrate of the grating. Typically, people do not specify carefully the groove spacing constancy of the grating or, alternatively, accept a large error because it is very difficult to measure the d-spacing along the whole grating surface with the needed precision.
Nevertheless we can estimate the effect of these errors on the resolving power and on the spot dimension after the grating.
The maximum achievable resolving power could be estimated (after equation 1) by:

$$\frac{\delta\lambda}{\lambda} = \frac{\frac{1}{n}(sin(\alpha) - sin(\beta))\delta d}{\frac{1}{n}(sin(\alpha) - sin(\beta))d} = \frac{\delta d}{d}$$

While the minimum spot dimension could be again obtained from equation 1 and is:

$$\delta S = \delta\beta \cdot r' = 2tg\beta \frac{\delta d}{d} r'$$

A different case is the one of the Variable Line Spacing (VLS) grating, where a groove density variation is required. The groove density K(*w*), along the direction *w* perpendicular to the grooves (centred on the pole of the grating), can be described via a polynomial series, i.e.

$$K(w) = K_0 + K_1 w + K_2 w^2 + K_3 w^3 + \cdots \qquad (3)$$

One should re-write the optical path function [2] and re-calculate the terms describing the focal property as well as the residual aberrations introduced by the grating. The general expression of these terms is:

$$F_{j00} = \frac{1}{2}\left(-n\lambda K_{j-1} + M_{j00}\right) \qquad (4)$$

Where M_{j00} are the terms describing the focal properties and the aberrations of the constant groove density gratings.
It's evident therefore that the polynomial terms K_1, K_2 and so on play a fundamental role in the prediction of the optical behaviour of the VLS gratings. Therefore, the knowledge of these terms is as important as the knowledge of the radius of curvature of a spherical grating or the knowledge of the residual slope errors.
Actually, the state of the art of the grating manufacturing is the following:
The slope errors of the blank could be reduced easily below 0.1 arcsec (0.5 µrad)
The groove density could be made up to 5000 l/mm without too many problems but could be also made larger
The groove density constancy is better then 0.01% ($\delta d/d$)
The dimension of an X-ray grating is not larger then 20 cm but typically lower.

Clamping induced deformations

One of the main problems, when a synchrotron beamline is designed, is to predict the real behaviours of the optical components under the operative conditions. Some problems arise from the high delivered power of third generation insertion device sources, due to the thermal induced deformations[1], to the growth of carbon compound on the optical surface[2], and to a general deterioration of the optics. Nevertheless, the necessity to align and cool the optics forces people to safely clamp the mirrors and the gratings on proper devices with the double purpose to move and cool them. Even if a lot of people does not mount the optics on real manipulators but prefer to move the whole vacuum chamber containing the mirror, it is, anyway, necessary to safely clamp them and, except if the mirrors are after the monochromator, they must be cooled. The cooling procedure could be direct or via copper braid, internal or external, made by water or cryogenically, on the edges or on the backside and so on. In any case a non-optical manufactured component tightly touch the optics, inducing a typically very small, but absolutely not negligible, deformation. The same concept could be applied to the problem of the clamping of a mirror to his manipulator. In this case a lot of tricks are adopted, trying to minimise the effect of the induced deformation due to the holders. By means of finite element calculation, is it possible to predict the ideal torque to apply to the screws or to the springs (and the position of them) to reduce, or ideally eliminate, the clamping induced deformations.
Nevertheless, at the end, the simulated conditions are never (or seldom) met. The small induced deformation could be large enough to drastically reduce the performances of a beamline, especially in the cases of high demanding energy resolving powers, small spot dimensions, and so on. In these cases, optics with less then 1 μrad rms slope errors in the tangential direction must be required and this small deviation, together with the desired shape, must be preserved under the operative conditions.
Some cases of clamping facility used in the synchrotron beamline are summarised in the following drawn.
The firsts two are different versions of the top-end clamping system. The force is applied on two antagonistic brackets to reduce the induced deformations. Two small wings are drawn in the mirror blank to further reduce the distortions. The typical distortion induced by this clamping system is an enlargement of the radius of curvature. If the original profile is a sphere with a radius lower than 100 m more or less, the effect is negligible alternatively it could be important.

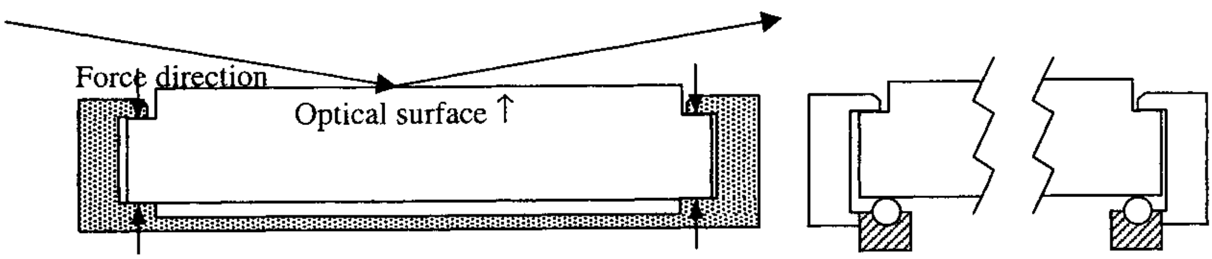

The next is facing down clamping system. The grating/mirror is supported by two lateral copper plates, which tightly hold the optics along its long edges. Two safety clasps are positioned along the short edges to avoid drops of the optics. The cooling plate could be positioned on the back or could be performed directly by the two copper plate used as brackets.
This kind of clamping system deform the mirror or the grating in the sagittal direction, without affect (or negligibly affect) the tangential direction

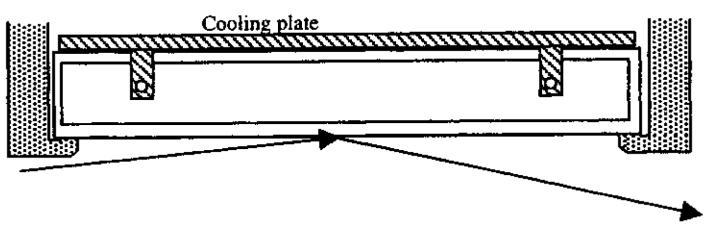

Another typical case is that one in which the mirror is lean on three (or five) rods and then clamped on them. This kind of clamping induces large distortion in the tangential direction if the force applied is too large and the rods are not positioned correctly.

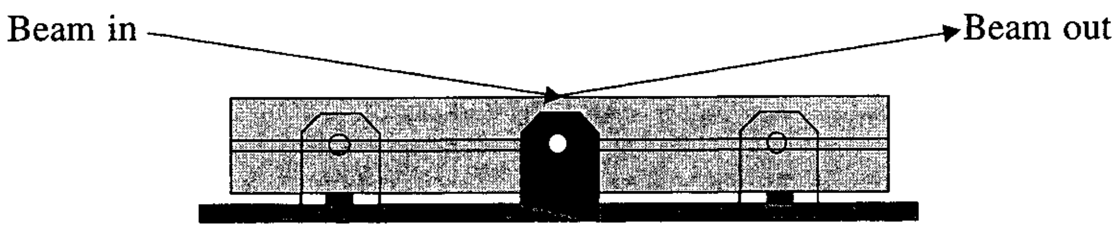

In any case it is clear that it is really difficult, or nearly impossible, to maintain unchanged the optical surface of a mirror after its clamping on the final holder, especially when a cooling system is to be applied. Nevertheless, it is possible to reduce the deformation to a "negligible" introduction of a radius of curvature of the order of several Kilometres. In the case of the soft X-ray mirrors, this effect could be not a problem, since the typical radius are of the order of some tens of meters, but in the cases of the Km range, this could be a real problem. An aid could be a clamping system that deforms the mirror only sagittally, but also in this case; a residual strain in the tangential direction is present. Another possible choice is to specify an optics surface better than the real needs. But this costs a lot of money that will be lost once the mirror is clamped. Nevertheless, it is a very good habit to measure, if possible, the mirrors after the final clamping. First of all, this could permit to reduce the deformations, and secondary, it reduces the possible source of uncertainty during the alignment procedure and therefore will save a lot of time.

In the following pages, some slide regarding the mirrors and the grating are included.

Basic principles

refractive index $\mu=1-\delta-i\beta$

$$\delta=(e^2\lambda^2/2\pi mc^2)|N+\Sigma_H N_H[\lambda/\lambda_H]^2\ln[\lambda_H^2/\lambda^2-1]|$$

δ (unit decrement) related to the speed in the medium

β related to the absorption

N=electron density (10^{23}-10^{24} el./cm^3)
λ_H=adsorption edge's wavelenght

λ far from $\lambda_H \Rightarrow \delta=Ne^2\lambda^2/2\pi mc^2$

$$\beta=\lambda\mu_l/4\pi$$

μ_l=linear absorption coefficient

VISIBILE

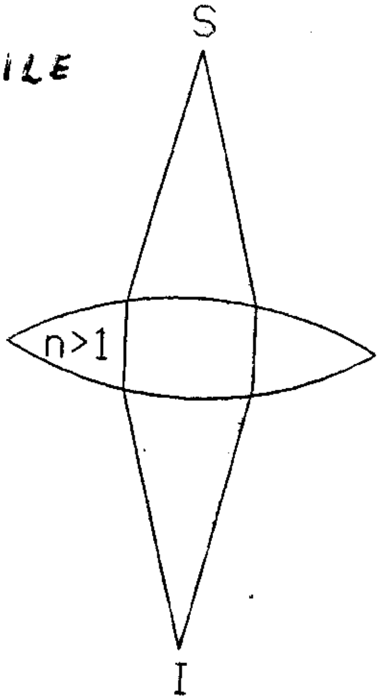

RAGGI X-MOLL

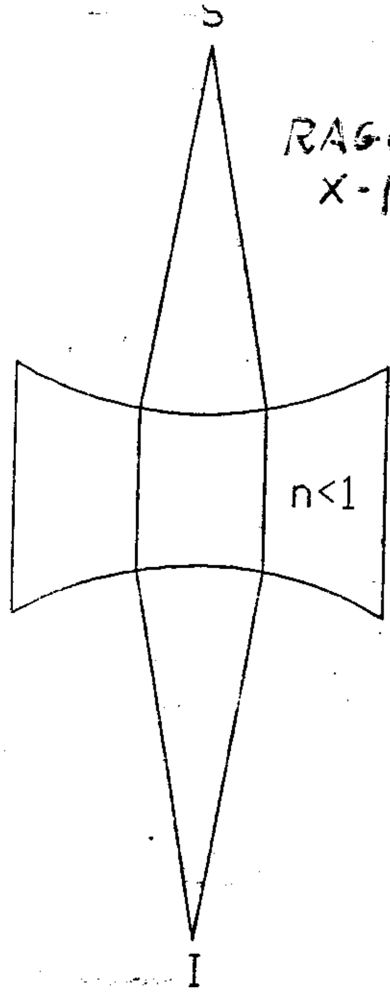

$$\delta = \frac{Ne^2\lambda^2}{2\pi mc^2} \simeq 10^{-4} \div 10^{-5}$$

$$\mu = 1 - \delta - j\beta$$

$$\frac{1}{f} = (n-1)\left(\frac{1}{R_1} + \frac{1}{R_2}\right) \Rightarrow$$

$n-1 \rightarrow 1-\delta-1$ (NEGATIVE); $\left(\frac{1}{R_1} + \frac{1}{R_2}\right) \rightarrow 2/R$

$$f = \frac{R}{2\delta}$$

$$\delta \simeq 10^{-5}$$

$$\Downarrow$$

per $R \simeq 1cm.$ $f \simeq 500mt.$

$$\Downarrow$$

$\delta \simeq 10^{-4}$ $R \simeq mm$

$$\Downarrow$$

$f = 1m.$ (HXR)

No refraction but reflection

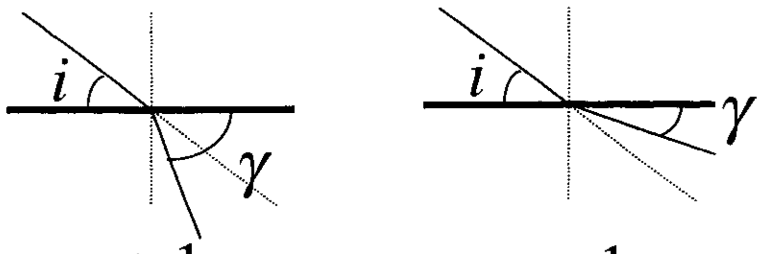

Snell's law: $\cos\gamma = \cos i / n$

$\gamma = 0 \quad n = \cos i_c$

ic critical angle: total external reflection

$\sin i_c = \lambda (e^2 N / \pi m c^2)^{1/2}$

$\lambda_c(\min) = 3.333 \cdot 10^{-13}\, N^{1/2} \sin i_c$

Material	Density (g/cm^3)	N ($electron/cm^3$)	λ_{min} nm
Pentadecane (oil)	0.77	$7x10^{22}$	64.1sin$i$
Glass	2.6	$78x10^{22}$	37.9sin$i$
Aluminum oxide	3.9	$115x10^{22}$	31.2sin$i$
Gold	19.3	$466x10^{22}$	15.4sin$i$

$i = 5^o$: λ_{min}glass=3.3nm=375 eV
λ_{min}gold=1.34nm=923eV

Synchrotron Radiation Beamline

Coupling as well as possible the source to the experiments

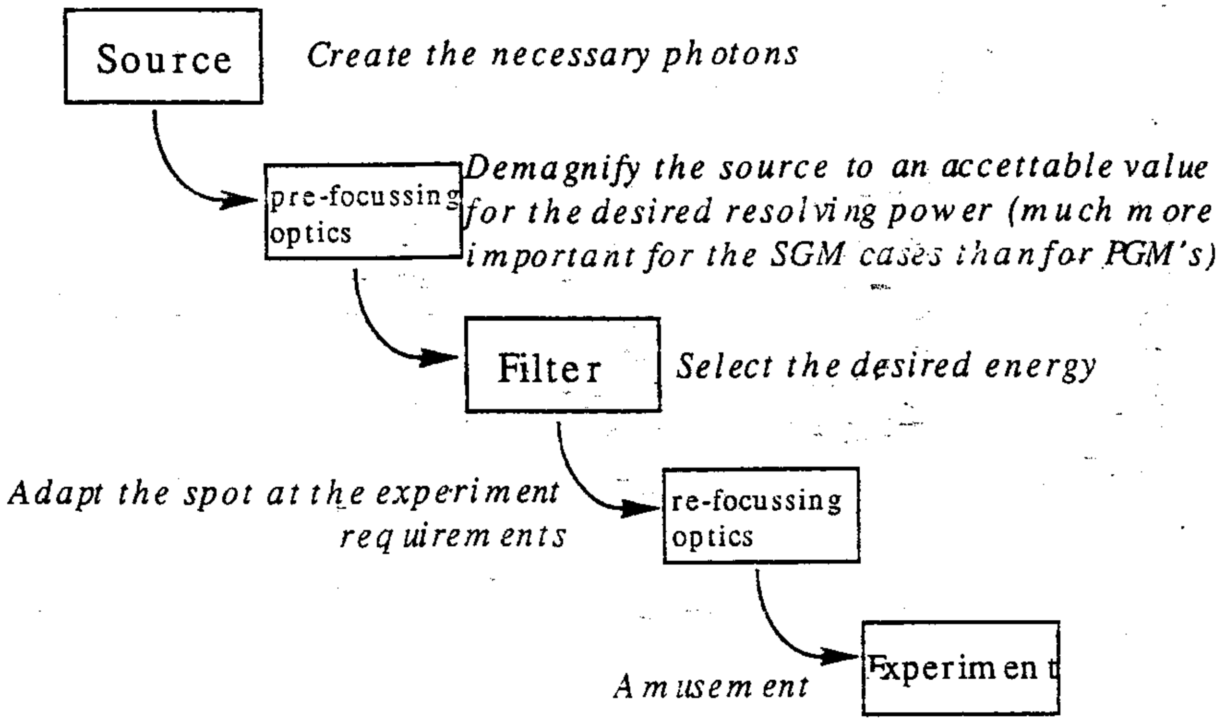

Strong absorption mean **Grazing incidence mirrors**

Wavelenght of the order of 1 10 nm mean **Diffraction gratings**

MIRRORS

Important parameter

Reflectivity
- Type of coating
- Angle of incidence

Shape — Aberrations introduced
- Elliptical
- Cylindrical
- Toroidal
- Plane
- Parabolic
- Spherical

Slope errors
- Long wavelenght (shape errors)
- medium wavelenght
- short wavelenght (roughness)

To be taken into consideration

Heat load effect
Carbon contamination
Mounting distortion
Mechanical tollerancies

Effect on the reflectivity of the carbon contamination

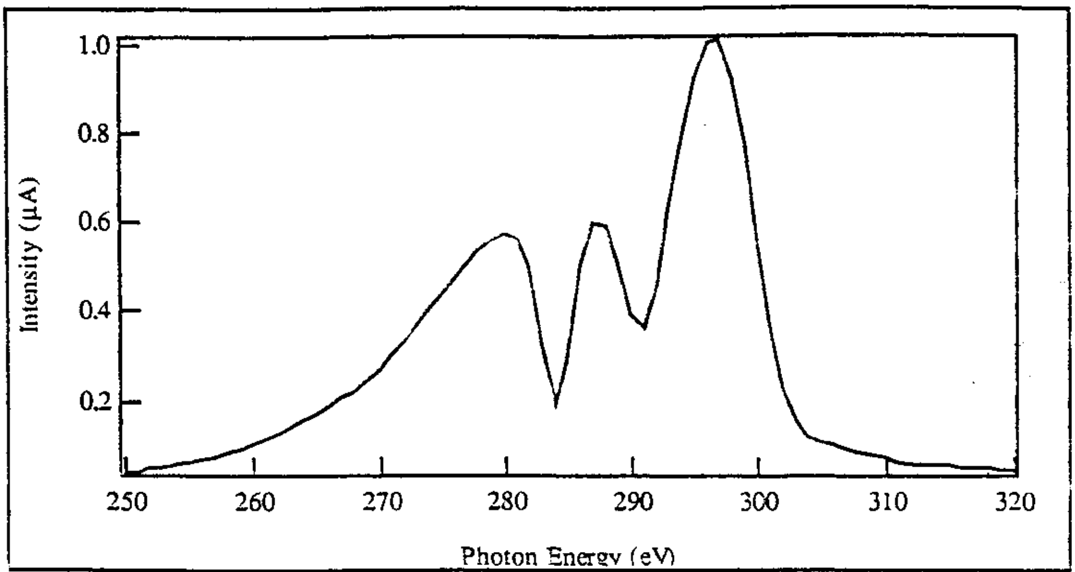

1st Harmonic Undulator spectra at the SuperESCA beamline July 1996

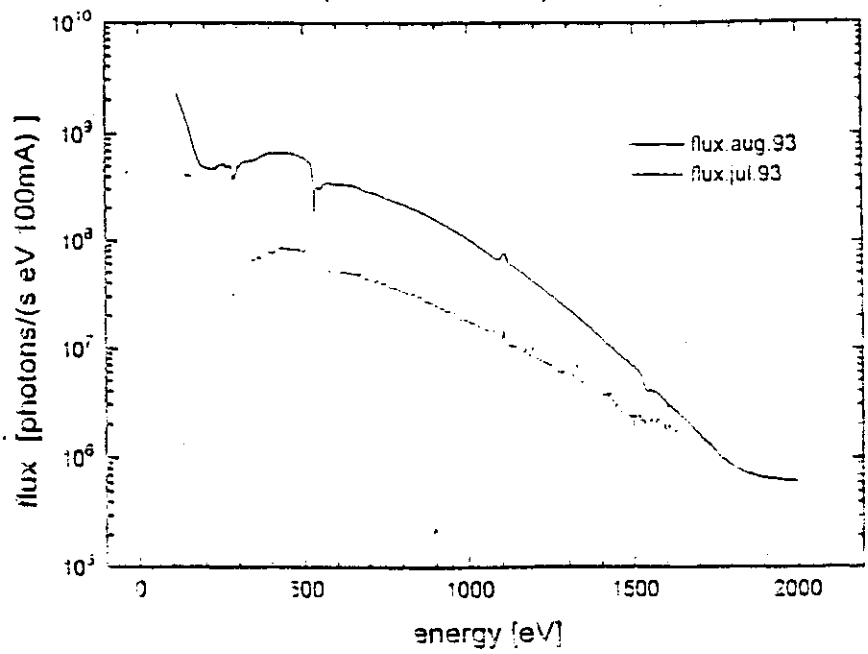

Fig. 3: Photon flux of the HE-PGM-3 beamline before and after plasma cleaning.

Contamination process

1) Hydrocarbons adsorbed by the surface
2) Cracking induced by the incoming radiation
3) Formation of graphitic carbon layer

Effect of the contamination

1) Strong absorption at the Carbon edge
2) Reduction of reflectivity at the higher energies
   (due to the different coating)
3) Enhancement of the surface roughness
4) Introduction of further slope errors
5) Overall deterioration of the performances

Cleaning Procedure

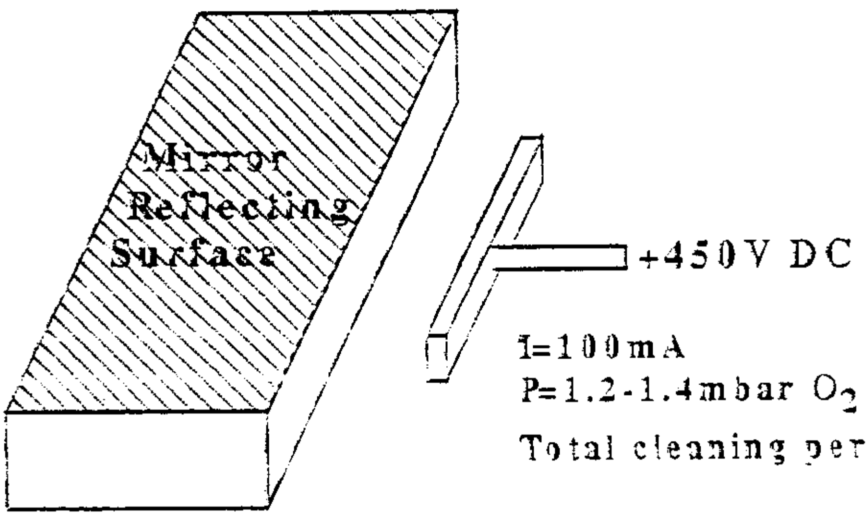

I=100mA
P=1.2-1.4mbar O_2
Total cleaning period=8-10h

Roughness Effect

$$R=R_0\, e^{-\left(\frac{4\pi\sigma \sin(\theta)}{\lambda}\right)^2}$$

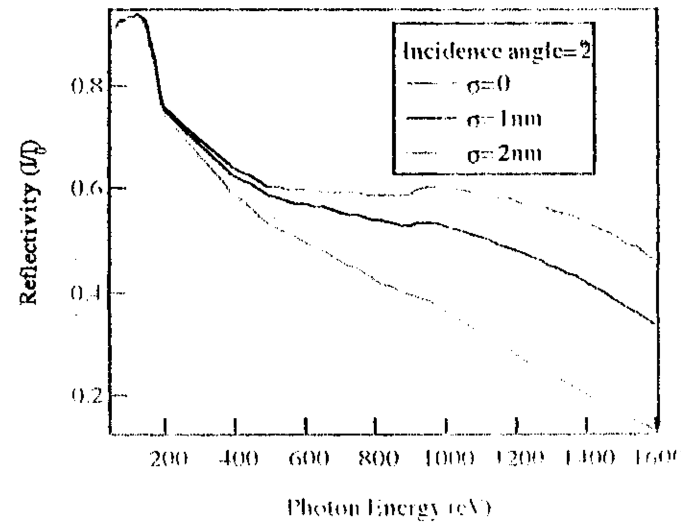

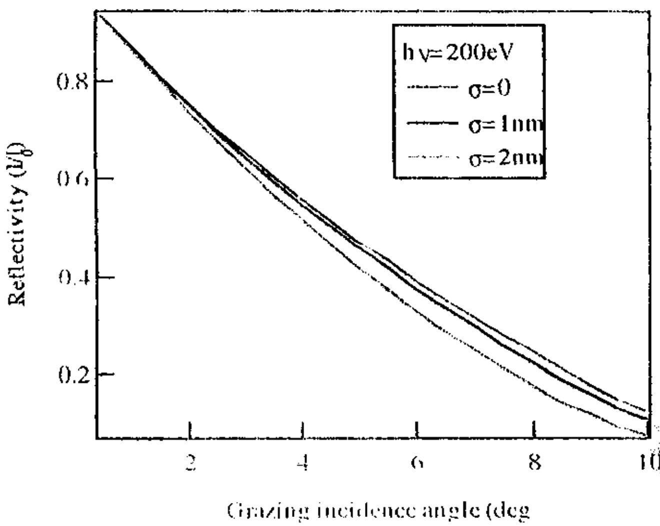

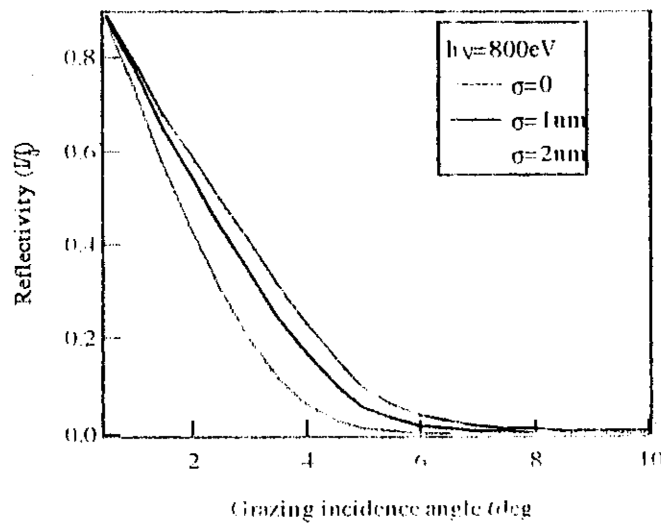

DISPERSIVE OBJECTS

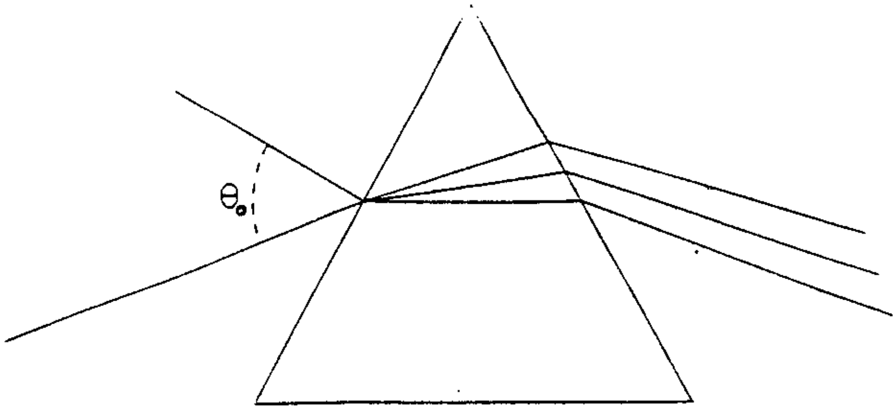

$$\frac{sen\theta_1}{sen\theta_0} = \frac{n_0}{n_1}$$ Visible

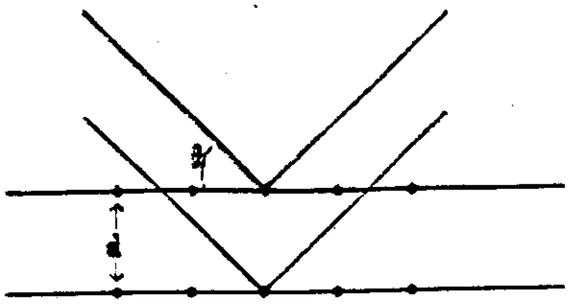

$$2sen\theta = \frac{n\lambda}{d}$$ Hard X-ray

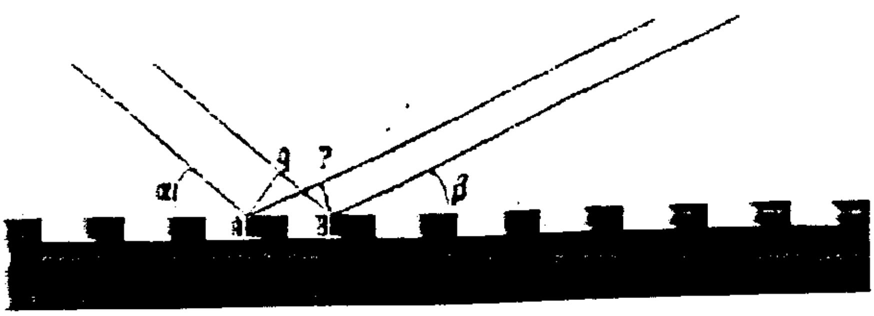

$$d\left(cos\beta - cos\alpha\right) = \lambda$$ Soft X-ray

Geometrical Aberation Theory

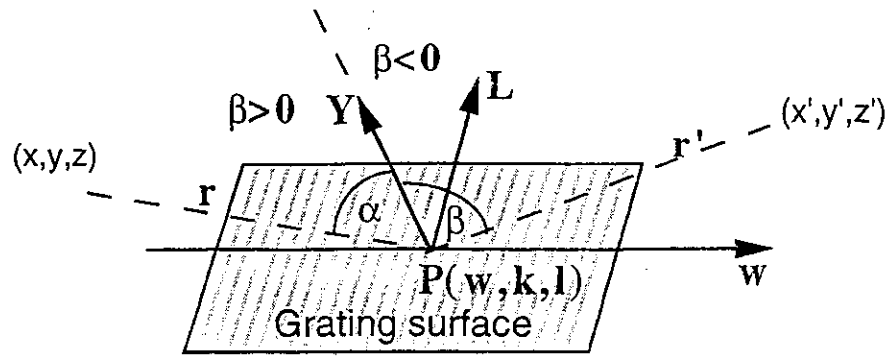

Dispersion equation $d(\sin\alpha - \sin\beta) = n\lambda$

Fermat's Principle ⟶ $\frac{\partial F}{\partial t} = 0$

$F = \overline{AP} + \overline{PB} + \frac{n\lambda}{d}$ Optical path

$\overline{AP} = \sqrt{(x-w)^2 + (y-k)^2 + (z-l)^2}$

$\overline{PB} = \sqrt{(x'-w)^2 + (y'-k)^2 + (z'-l)^2}$

Minimum time = Minimum distance

↓ (If in the same medium)

$\frac{\partial F}{\partial w} = 0 \;;\; \frac{\partial F}{\partial l} = 0 \qquad k = \sum_{i,j} K_{ij} w^i l^j$

Re-written the optical path function as a function of the known parameters:

$x = -r \cdot \cos\alpha \quad y = r \cdot \sin\alpha \quad x' = r'\cos\beta \quad y' = r'\sin\beta \quad z' = -z\frac{r'}{r}$

III HOLOGRAPHICALLY RECORDED DIFFRACTION GRATINGS (H.R.D.G.)

A Production flow chart of H.R.D.G.

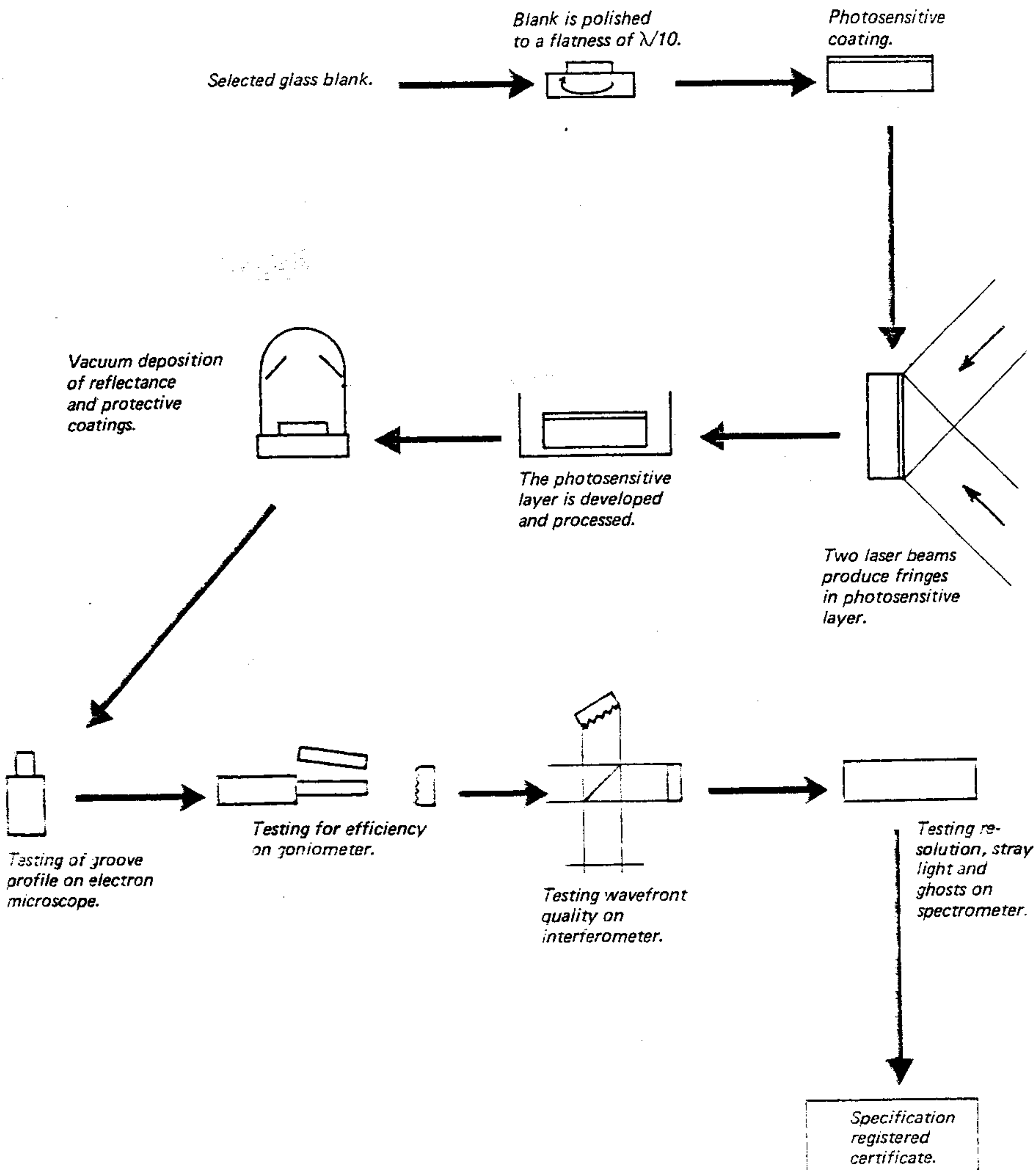

Fig. 3-1 Production flow chart for holographic gratings.

3

Effect of a non-uniform groove density

Long wavelength errors

Manufacturing errors

$$\frac{\delta\lambda}{\lambda}=\frac{\frac{1}{n}(\sin(\alpha)-\sin(\beta))\delta d}{\frac{1}{n}(\sin(\alpha)-\sin(\beta))d}=\frac{\delta d}{d}$$

Maximum resolving power?

$$\delta S=\delta\beta\cdot r'=2tg\beta\frac{\delta d}{d}r'$$

Minimum spot dimension?

Ghosts & Stray Light

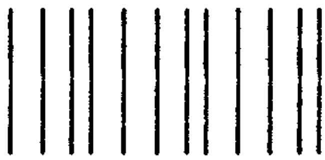

Periodic imperfections

$$I_g=I_0\left(\frac{n\pi\,\delta d}{d}\right)^2$$

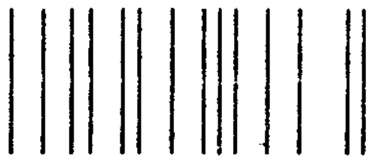

Random imperfections

$$I=I_0\exp-\left(\frac{2\pi\,\sin\beta\,\delta d}{\lambda}\right)$$

δd

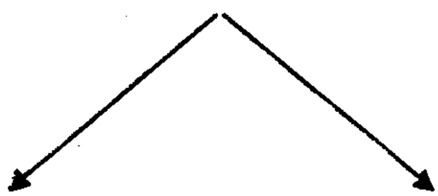

Maximum deviation from the ideal d-spacing

rms deviation from the ideal d-spacing

VLS gratings

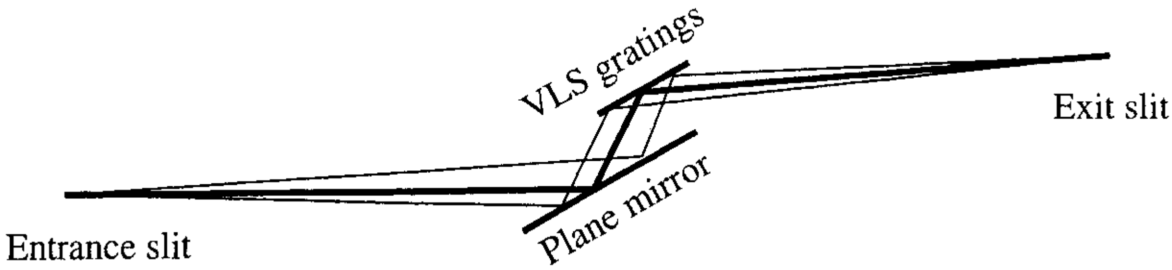

$$K(w) = K_0 + K_1 w + K_2 w^2 + K_3 w^3 + \cdots$$

$$F_{100} = -n\lambda K_0 + (sin\alpha - sin\beta)$$

$$F_{200} = \frac{1}{2}(-n\lambda K_1 + M_{200}) \quad \Rightarrow \quad -n\lambda K_1 + \frac{\cos^2\alpha}{r} + \frac{\cos^2\beta}{r'} = 0$$

$$F_{300} = \frac{1}{3}\left(-n\lambda K_2 + \frac{3}{2}M_{300}\right) \quad \Rightarrow \quad -n\lambda K_2 + \frac{3}{2}\left(\frac{\sin\beta \quad \cos^2\beta/}{r'} - \frac{\sin\alpha \quad \cos^2\alpha/}{r}\right)$$

$$\vdots$$

Reduction of higher order aberrations

Focusing plane gratings

Constant demagnification ratio of plane VLS monochromators

Increasing of focusing property of spherical gratings

Diffraction grating's properties

Magnification

$$M(\lambda) = \frac{s'}{s}$$

s=source dimension

s'=image dimension

$$Nk\lambda = sin(\alpha) - sin(\beta)$$

→ $$\left(\frac{\partial\lambda}{\partial\alpha}\right) = \frac{\cos(\alpha)}{Nk} \qquad \Delta\alpha = \frac{s}{r}$$

→ $$\left(\frac{\partial\lambda}{\partial\beta}\right) = \frac{\cos(\beta)}{Nk} \qquad \Delta\beta = \frac{s'}{r'}$$

$$M(\lambda) = \frac{s'}{s} = \frac{r' \ \cos(\alpha)}{r \ \cos(\beta)}$$

Resolving Power

$$\Delta\lambda_{entrance} = \frac{s \cdot \cos(\alpha)}{Nkr}$$

entrance slit contribution

$$\Delta\lambda_{exit} = \frac{s' \cdot \cos(\beta)}{Nkr'}$$

exit slit contribution

$$\Delta\lambda_0 = \frac{\lambda}{2Nkw_0}$$

diffraction limited

Diffraction grating's efficiency

Blaze profile

Laminar profile

VLS Spherical grating spectrometer

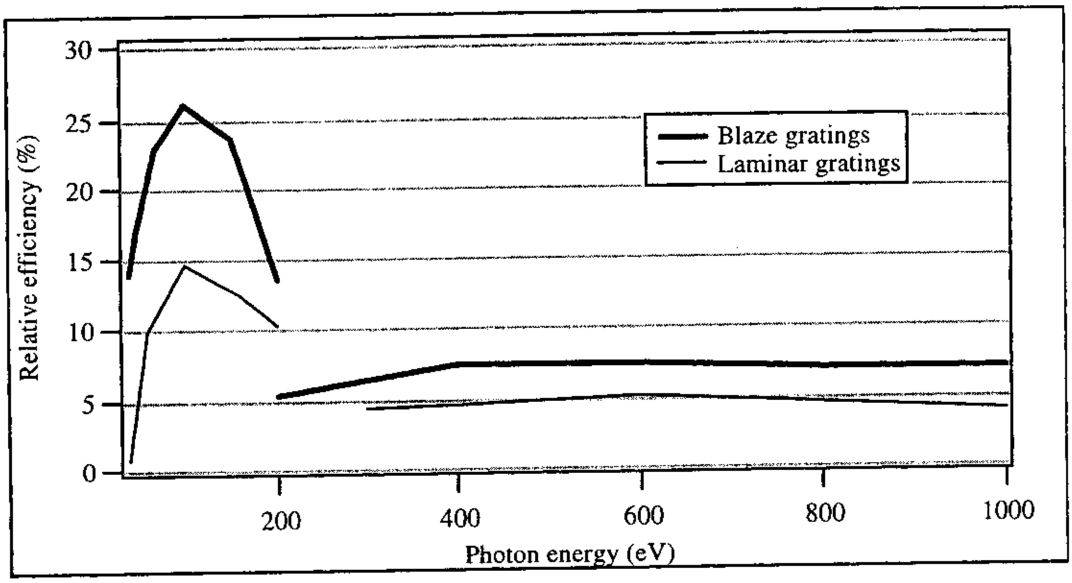

VLS Plane grating monochromator

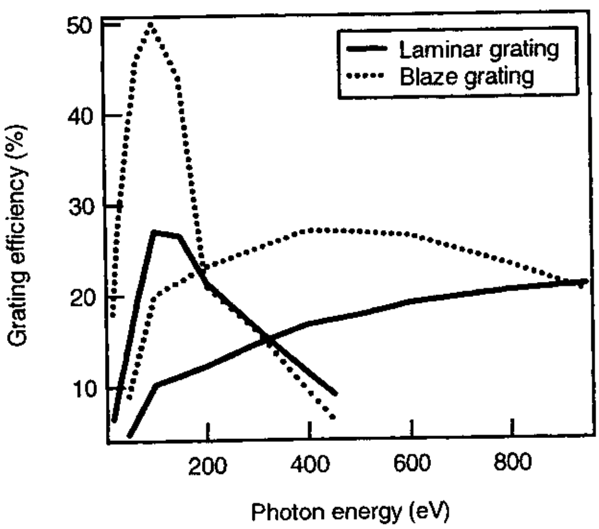

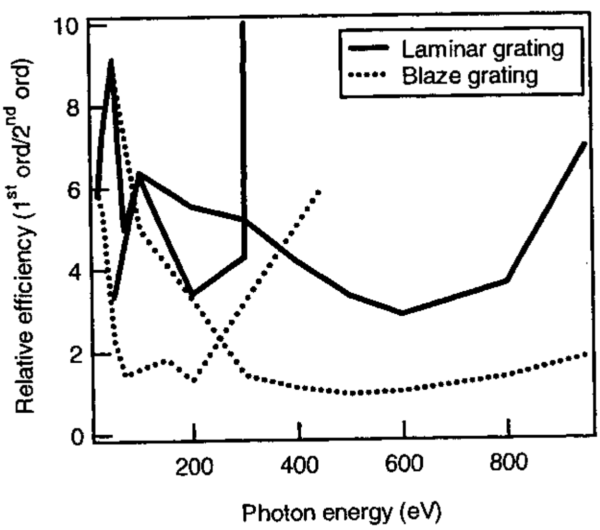

Grating simulation parameters:

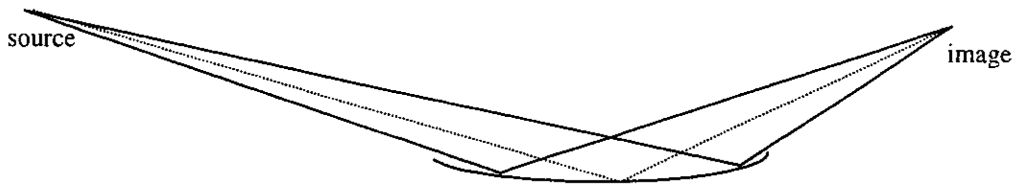

Parameter	Value
SOURCE	
Spatial type	Gaussian
spatial sigma x,z	240μm,10μm
angular sigma (vertical,horizontal)	100μrad,100μrad
photon energy	100 eV, **500eV**
GRATING	
Shape	Spherical
Radius of curvature	2000 cm
groove density	6000 l/mm
distance source grating	400 cm
distance grating image	150 cm
incidence angle	80.94452 , **83.04834**
diffraction angle	84.25400 , **83.7923**
diffraction order	internal, i.e. +1